An ALE-based method for reaction-induced boundary movement towards clogging

K. Kumar[1], T. L. van Noorden[2] M. F. Wheeler[3], and T. Wick[4]

[1] The University of Texas at Austin, Center for Subsurface Modeling, The Institute for Computational Engineering and Sciences, Austin, Texas 78712, USA, `kkumar@ices.utexas.edu`
[2] Comsol B.V., Zoetermeer, The Netherlands `t.l.v.noorden@gmail.com`
[3] The University of Texas at Austin, Center for Subsurface Modeling, The Institute for Computational Engineering and Sciences, Austin, Texas 78712, USA, `mfw@ices.utexas.edu`
[4] The University of Texas at Austin, The Institute for Computational Engineering and Sciences, Austin, Texas 78712, USA, `twick@ices.utexas.edu`

Abstract. In this study, reaction-induced boundary movements in a thin channel are investigated. Here, precipitation-dissolution reactions taking place at the boundaries of the channel resulting in boundary movements act as a precursor to the clogging process. The resulting problem is a coupled flow-reactive transport process in a time-dependent geometry. We propose an ALE-based method (ALE - arbitrary Lagrangian-Eulerian) to perform full 2D computations. We derive a 1D model that approximates the 2D solution by integrating over the thickness of the channel. The boundary movements lead in the limit to clogging when the flow gets choked for a given pressure gradient applied across the channel. Numerical tests of the full 2D model are consulted to confirm the theory.

1 Motivation

Reactive flows are of great importance in a variety of fields including but not limited to porous media, biomedical applications, and biofilm growth [2,3,7,8,6]. Reactive processes such as precipitation-dissolution lead to geometry changes leading to changes in the flow which in turn affects the transport. Hence, the resulting model must consider geometry changes, reactive processes, transport and flow problems in a coupled manner. In this work, we consider flow in a thin channel where ions are transported by flow and undergo molecular diffusion. The ions react to each other at the boundaries of the channel leading to the deposition of the crystalline material. We consider both the precipitation and dissolution processes as prototypes of reactions. The particularity is in the reactions, namely, precipitation and dissolution processes taking place at the boundaries of the channel leading to the deposition of the crystal material.

We employ an ALE-based method (ALE - arbitrary Lagrangian-Eulerian) to study coupled flow-transport phenomena in a time-dependent geometry. The initial geometry is quite simple and taken to be a thin channel which is a representative pore scale geometry. The changes in the geometry, as already stated, result from the reactions which are themselves functions of concentration and geometry. Hence,

the time-dependent configuration remains an unknown and hence part of the solution variable. Since full 2D computations for the channel are expensive, we consider a 1D upscaled model derived in [5]. Both the 2D model and its approximate 1D model predict decreasing of strength of the flow as the channel progressively gets narrower. We term the limit of the narrowing of the channel as clogging, which is consistent with the intuitive notion.

The ALE method presented in this paper has been discussed in detail in [4] whereas the upscaled 1D model has been derived in [5] for a different set of boundary conditions for flow. We consider pressure boundary conditions for the flow which allows us to investigate the choking of the flow when the channel becomes constricted. These earlier studies did not consider the clogging process due to their choice for the boundary conditions for the flow. Our motivation for the present investigation stems from studying processes preceding the clogging and its effect on the flow and transport and further being able to define both 2D and upscaled 1D equations describing the behavior of *post-clogging*. Consequently, this work is a beginning in this direction.

The outline of the article is as follows: In Section 2, we recapitulate the underlying partial differential equations for the thin strip. Then, in Section 3, we state a 1D upscaled model. Next, the ALE method and discretization schemes for solving the free and moving boundary problem in the thin strip are described in Section 4. It is followed by Section 5 where clogging is discussed. Finally, in Section 6, the numerical experiments are conducted for full 2D model and we conclude by commenting on the consistence of 1D model with full 2D computations.

2   Equations

Let Ω_0 be a bounded domain in $\mathbb{R}^2$ representing a thin strip. The region occupied by the flow is $\Omega(t) \subset \Omega_0$, the precipitate layer is described by $\Gamma(t)$, with the inlet and outlet denoted by Γ_i and Γ_o. The geometry description in which the flow and transport processes take place is given by:

$$
\begin{aligned}
\Omega(t) &:= \{(x,y) \in \mathbb{R}^2 \mid 0 \leq x \leq 1, \ -(\varepsilon - d(x,t)) \leq y \leq (\varepsilon - d(x,t))\}, \\
\Gamma(t) &:= \{(x,y) \in \mathbb{R}^2 \mid 0 \leq x \leq 1, \ y \in \{-(\varepsilon - d(x,t)), (\varepsilon - d(x,t))\}\}, \\
\Gamma_i(t) &:= \{(x,y) \in \mathbb{R}^2 \mid x = 0, \ -(\varepsilon - d(0,t)) \leq y \leq (\varepsilon - d(0,t))\}, \\
\Gamma_o(t) &:= \{(x,y) \in \mathbb{R}^2 \mid x = 1, \ -(\varepsilon - d(1,t)) \leq y \leq (\varepsilon - d(1,t))\}.
\end{aligned}
$$

Due to the reactions at the boundaries, Ω and the boundaries Γ's are time-dependent. The schematic illustration for the thin strip is displayed in Figure 1.

The flow and transport of the solutes (the ions) are described by the following system of equations. The transport equation reads:

$$
\begin{aligned}
\partial_t c &= \nabla \cdot (D\nabla c - vc), & &\text{in} \ \ \Omega(t) \times (0,T), \\
\rho_s \partial_t d &= f(c, \rho_s d)\sqrt{1 + (\partial_x d)^2}, & &\text{on} \ \ \Gamma(t) \times (0,T), \\
f(c, \rho_s d) &= r(c) - w, & &\text{on} \ \ \Gamma(t) \times (0,T).
\end{aligned}
\tag{1}
$$

Here, the unknowns are: $c(x,y,t)$, concentration of the charged ions, $d(x,t)$ free and moving boundary resulting due to reactions, and $v(x,y,t)$ the flow field. The known physical parameters are: $D > 0$, diffusion constant, ρ_s, the density of ions in the precipitate. $(1)_1$ describes the transport of solutes due to convection and molecular
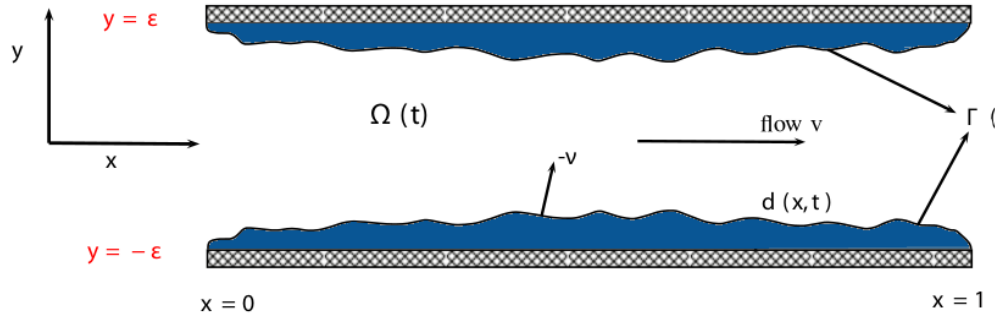
Fig. 1. Schematic of a thin channel showing the geometry changes due to precipitate being formed at the boundaries. The flow and transport takes place in $\Omega(t)$ and the reactions take place at lateral boundaries $\Gamma(t)$.

diffusion processes, whereas $(1)_2$ describes the movement of the boundary due to reaction term f. According to $(1)_3$, the reaction rate f is imposed by the following structure:

$$f(c, \rho_s d) = r(c) - w, \tag{2}$$

where $r(\cdot)$ describes the precipitation part whereas w models the dissolution process. Additionally, we assume that $r(\cdot) : \mathbb{R} \to [0, \infty)$, is monotone and locally Lipschitz continuous in $\mathbb{R}$. The usual mass-action kinetics laws governing the precipitation process satisfy this assumption. For the dissolution process, the rate law is given as

$$w \in H(d), \quad \text{where} \quad H(d) = \begin{cases} \{0\}, & \text{if} \quad d < 0, \\ [0, 1], & \text{if} \quad d = 0, \\ \{1\}, & \text{if} \quad d > 0. \end{cases} \tag{3}$$

The flow equations read:

$$\begin{aligned} \text{Continuity:} \quad & \nabla \cdot v = 0, && \text{in} \quad \Omega(t) \times (0, T), \\ \text{Momentum:} \quad & \rho_f v \cdot \nabla v = \nabla \cdot \left(\mu_f (\nabla v + (\nabla v)^T) \right) - \nabla p, && \text{in} \quad \Omega(t) \times (0, T), \end{aligned} \tag{4}$$

where p is the pressure field and $\mu_f = \rho_f \nu_f$ is the dynamic viscosity. The flow and transport equations are complemented by the initial and boundary conditions. The initial conditions read:

$$c(x, y, 0) = c_o, \qquad d(x, 0) = d_o. \tag{5}$$

The boundary conditions read:

$$\begin{aligned} c &= c_b, & p(0, y, t) &= 1, & \text{on} \quad & \Gamma_i(t) \times (0, T), \\ \partial_x c &= 0, & p(L, y, t) &= 0, & \text{on} \quad & \Gamma_o(t) \times (0, T), \\ v &= 0, \;\; \nu \cdot (-D\nabla c)\sqrt{1 + (\partial_x d)^2} = \partial_t d(\rho_s - c) & & & \text{on} \quad & \Gamma(t) \times (0, T). \end{aligned} \tag{6}$$

As stated above, at the inlet and outlet, we prescribe the pressures and further impose that the flow takes place normal to the boundaries.

3   A 1D averaged model

An upscaled model is obtained by integrating the equations in the y-direction. We consider a sequence of problems depending upon the thickness of strip ε and using formal asymptotic expansions, the unknowns are assumed to be of the form

$$z^\varepsilon = z_0 + \varepsilon z_1 + O(\varepsilon^2),$$

with z^ε denoting any of $c^\varepsilon, d^\varepsilon, v^\varepsilon$. Following the procedure in [5], the following upscaled equations are derived

$$\partial_x v_0 = 0, \qquad v_0 - \frac{(1-d_0)^3}{3\mu}\partial_x P_0 = 0,$$
$$\partial_t\left((1-d_0)c_0\right) + \partial_t(\rho_s d_0) \qquad = \partial_x\left(D(1-d_0)\partial_x c_0\right) - \partial_x(v_0 c_0), \qquad (7)$$
$$\partial_t d_0 - f(u_0, \rho_s d_0) \qquad = 0.$$

As our interest is in the case of closing of the channel, the above system of equations degenerates as $d_0 \to 1$. In this work, we consider only the flow equations, that is, $(7)_1$. The limit case for the reactive transport will be treated in future studies.

4   ALE based method for full thin-strip computations and discretization

The moving boundary problem is computed with the help of the arbitrary Lagrangian-Eulerian (ALE) approach that is mostly well-known from fluid-structure interaction computations. Here, rather than computing the equations on the physical mesh (bottom figure in Figure 2), the equations are solved on a reference mesh (top figure in Figure 2) by transforming them with the ALE-mapping. The discretization is based on Rothe's method: first in time and than in space. A one-step-θ scheme is employed for temporal discretization and a Galerkin finite element method for spatial discretization including local mesh refinement with hanging nodes. Since we are solving the incompressible Navier-Stokes equations and due to the ALE-mapping, we deal with a nonlinear system of equations, which is solved in a monolithic fashion. The linear equations are treated with a direct solver. Rather than providing all necessary information and all important references of this section, we would like to refer the friendly reader to [4], where all details are given. The discretization is realized with the multiphysics template [10] based on the finite element software deal.II [1].
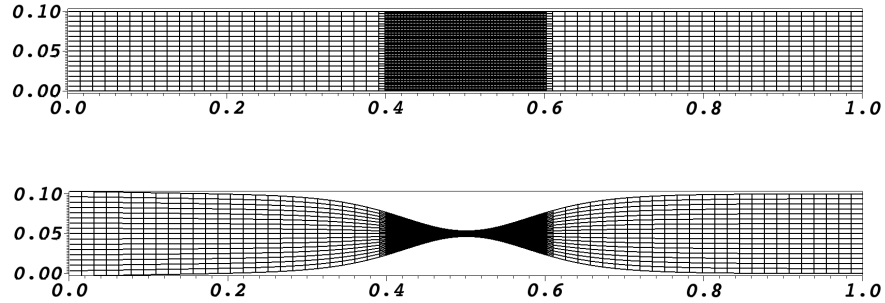
Fig. 2. Initial (and also the reference) mesh and the deformed mesh at end time step $T = 14$. Local mesh refinement with hanging nodes is used in the middle of the channel.

5   Clogging of the channel

When the channel starts getting narrower, the flow profile alters because of changing geometry. However, as the channel starts getting clogged, the flow is expected to decrease and eventually, the channel should be closed. For the upscaled model, following calculations show that the flow becomes zero as the channel closes. Using $(7)_1$

$$\partial_x \left(\frac{(1-d_0)^3}{3\mu} \partial_x P_0 \right) = 0, \text{ leading to } \frac{(1-d_0)^3}{3\mu} \partial_x P_0 = C,$$

and hence,

$$P_0(x,t) = \int_x^1 \frac{C}{(1-d_0(\xi,t))^3} d\xi,$$

where C is obtained by using the boundary conditions for P_0,

$$v_0(t) = C(t) = \left\{ \int_0^1 \frac{1}{(1-d_0(\xi,t))^3} d\xi \right\}^{-1}. \tag{8}$$

Now considering (8), formally, one sees that the integral is dominated by the regions where $1 - d_0$ is small and the flow $v_0(t)$ decreases as $(1 - d_0)^3$. Hence, wherever locally $d_0 \to 1$, we get that the flow in the channel tends to zero, allowing us to conclude that in the limit (clogging), the flow becomes zero. Since the 2D model is quite complicated, an analytical treatment is rather difficult. We resort to numerical computations to study this process in the following section.

6   Numerical tests

We conduct numerical tests using the full 2D model and study the pressure and flow profiles. These 2D tests are based on the second numerical example presented in [4]. Specifically, we have a right-hand side force function (representing an analytical expression for a point source)

$$f(x,y) = a \exp(-b(x - x_m)^2 - c(y - y_m)^2),$$

where $a = 1000, b = c = 100$ and $x_m = 0.5, y_m = 0.05$, representing a source with maximum strength at (x_m, y_m) and having an exponential decay and causing the precipitation in the middle of the thin channel $\Omega := [0,1] \times [0, 0.1]$. All material parameters and geometry information are described in the previously mentioned article [4]. In contrast, the flow is now driven by pressure difference such that we have $p = 1$ on the inflow (left boundary) and $p = 0$ at the right (outflow) boundary. The initial concentration is $c = 1$ for all $x \in \Omega$. In addition, we prescribe $c = 0$ at the left boundary. The goal of our present study is now different from [4]. We are specifically interested in the pressure behavior along the x-axis and the validity of approximating the behavior through the lower-dimensional lubrication equation $(7)_1$.
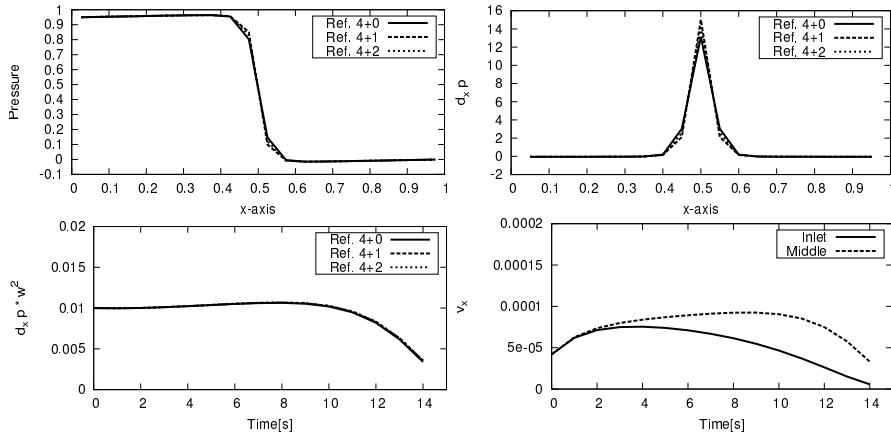

Fig. 3. Results of the 2D numerical simulation: Profiles at final time $T = 14$ for the pressure, its gradient, and the key observation quantity $\partial_x p w^2$ shown in the first three figures. Each of the quantities of interest is computed on a sequence of three locally refined meshes to have numerical evidence of convergence. In the final figure, the velocity component in normal flow direction integrated over the cross section is shown on the finest mesh for the inlet and the middle (narrow part of the channel).

Figure 3 shows the pressure and the pressure gradient at $T = 14$ when the channel has closed by ≈ 92 percent. Furthermore, the two bottom figures show $w^2 \partial_x p$ (w is the width of flow domain) and the v_x velocity with respect to time. The choice of this scaling w^2 is motivated by considering (7) $_1$; since the total flow follows the cubic law, the average flow obeys a square law. For the 2D model, achieving the limit is not possible since the mesh will degenerate as the channel is closed. (This drawback in the numerics is investigated in terms of a standard fluid-structure interaction framework in [9]). However, the amount of channel constriction is pretty close to the process of clogging. The profile shows that the pressure gradients are blowing up as the channel gets smaller. However, when this is weighted with $2(\varepsilon - d)^2$, that is with square of the opening width of the channel, the resulting quantity goes to zero. This quantity is proportional to the flow and showing similar behavior as displayed in Figure 3. This suggests that the flow strength vanishes as the channel progressively gets clogged. This is consistent with the case of upscaled model. Figure 4 displays the plot of concentration for two different times.
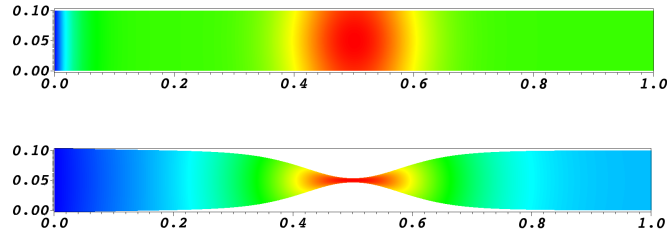

Fig. 4. Results of the 2D numerical simulation: Concentration at the first time step and the end time step $T = 14$. At the initial time, the concentration is $c = 1$ in the whole channel. Starting the simulation, $c = 0$ is applied at the inlet boundary (blue) and the source term f increases the concentration in the middle (red).

7   Conclusion

In this work, we investigated a coupled flow-reactive transport model in a time-dependent thin channel where the geometry changes are induced by reactive boundary conditions. The 2D model is solved using ALE-based method. A pressure gradient is applied across the channel and as the channel gets constricted, the flow strength diminishes so that in the limit we get no-flow across the channel. The approximating 1D model can be analytically studied and formal arguments are employed to obtain the same observations. The study highlights that a local clogging leads to the closing (in the sense of flow) of the channel. In addition, this study provides some hints that the derived 1D upscaled model with appropriate boundary conditions will allow us to capture the clogging phenomenon and continue the solution thereafter. The findings of this work serve as precursor for future studies of post-clogging processes.

Acknowledgment

References

1. W. BANGERTH, T. HEISTER, AND G. KANSCHAT, *Differential equations analysis library*, 2012.

2. S. ČANIĆ AND A. MIKELIĆ, *Effective equations modeling the flow of a viscous incompressible fluid through a long elastic tube arising in the study of blood flow through small arteries*, SIAM J. Appl. Dyn. Syst. **2**:3 (2003), 431–463 (electronic).

3. C. D'ANGELO AND P. ZUNINO, *Robust numerical approximation of coupled Stokes' and Darcy's flows applied to vascular hemodynamics and biochemical transport*, M2AN **45** (2011), 447–476.

4. K. KUMAR, M. WHEELER, AND T. WICK, *Reactive flow and reaction-induced boundary movement in a thin channel*, accepted in SIAM J. Sci. Comput., 2013.

5. T. L. v. NOORDEN, *Crystal precipitation and dissolution in a thin strip*, European J. Appl. Math. **20**:1 (2009), 69–91.

6. T. L. v. NOORDEN, I. S. POP, A. EBIGBO, AND R. HELMIG, *An upscaled model for biofilm growth in a thin strip*, Water Resour. Res. **46**:W06505 (2010).

7. A. QUARTERONI, A. VENEZIANI, AND P. ZUNINO, *A domain decomposition method for advection-diffusion processes with application to blood solutes*, SISC **23**:6 (2002), 1959–1980.

8. _____ , *Mathematical and numerical modeling of solute dynamics in blood flow and arterial walls*, SINUM **39**:5 (2002), 1488–1511.

9. T. RICHTER AND T. WICK, *Solid growth and closure in fluid-structure interaction computed in ALE and fully Eulerian coordinates*, Preprint, 2013.

10. T. WICK, *Solving monolithic fluid-structure interaction problems in arbitrary Lagrangian Eulerian coordinates with the deal.ii library*, Archive of Numerical Software **1** (2013), 1–19.